Structural and spectroscopic characteristics of neodymium doped $CaTa_2O_6$ single crystal fibres grown by the laser heated pedestal growth technique

2004 J. Phys.: Condens. Matter 16 5915

(http://iopscience.iop.org/0953-8984/16/32/024)

INSTITUTE OF PHYSICS PUBLISHING JOURNAL OF PHYSICS: CONDENSED MATTER

J. Phys.: Condens. Matter **16** (2004) 5915–5923 PII: S0953-8984(04)81026-9

Structural and spectroscopic characteristics of neodymium doped $CaTa_2O_6$ single crystal fibres grown by the laser heated pedestal growth technique

A S S de Camargo[1], C R Ferrari, A C Hernandes and L A O Nunes

Instituto de Física de São Carlos, Universidade de São Paulo—USP, CP 369, CEP 13560-970, São Carlos—SP, Brazil

E-mail: andreasc@if.sc.usp.br

Received 19 May 2004
Published 30 July 2004
Online at stacks.iop.org/JPhysCM/16/5915
doi:10.1088/0953-8984/16/32/024

Abstract

We report the successful growth of undoped and neodymium doped $CaTa_2O_6$ single crystal fibres by the laser heated pedestal growth (LHPG) technique, as well as the fibres' structural and spectroscopic characterizations. The 700 μm diameter and 3 cm length fibres present high optical quality and excellent transparency, and x-ray diffraction measurements indicate that they crystallize in the cubic structure ($Pm3$). The extensive transmission window of the host crystal fibres enables the study of rare-earth ion emission in the near-infrared region with several technological applications. Neodymium doped fibres (0.5–2.5 mol%) were characterized by ground and excited state absorptions, luminescence and lifetime measurements. Stimulated emissions were measured at 1.06 μm ($^4F_{3/2} \rightarrow {}^4I_{11/2}$ transition) and around 1.34 μm ($^4F_{3/2} \rightarrow {}^4I_{13/2}$). Because $CaTa_2O_6$:Nd^{3+} fibres can be grown with excellent optical quality at low cost and in processes that are much faster than those usually used to grow bulk crystals, they might become an interesting material for the construction of compact optical devices such as diode pumped miniature lasers.

1. Introduction

Nowadays, solid state materials presenting emissions in the near infrared spectral region (1–3 μm), are highly desirable for the construction of optical and electro-optical devices such as detectors, amplifiers, laser active media, etc, with applications in the scientific, military, industrial and medical fields [1–5]. Consequently, there is an enormous interest in the development and improvement of new and efficient materials, and among them the rare-earth ion doped crystals play a major role. In particular, neodymium doped crystals that can be

[1] Author to whom any correspondence should be addressed.

used as laser active media around 1.06 and 1.34 μm are probably the most studied ones. The emission at 1.06 μm finds applications in optical spectroscopy and dentistry (for the removal of cariotic tissue for instance), and the one at 1.34 μm is studied due to the possibility of application in amplifiers for telecommunications [4, 5].

Although several crystal compositions have been studied for the last forty years, most of the spectroscopic investigations and laser experiments reported in the literature are carried out in large bulk crystals, obtained by expensive and sophisticated techniques such as the Czochralski method [6, 7]. More recently however, the demand for compactness of optical devices has raised much attention for the preparation and characterization of single crystal fibres [8–12], which give perspective for the construction of low cost and mass producible devices, such as miniature lasers. One of the interesting features of these lasers are the fact that, since their cavity length can be made sufficiently short, single mode oscillation can be achieved, assuring single-frequency output, and it is much easier to stabilize a short cavity to minimize thermal and mechanical perturbations [13].

A technique that has been successfully used for the growth of high optical quality single crystal fibres of various compositions is the laser heated pedestal growth (LHPG) technique [8, 14]. This is a modified floating zone technique in which the molten zone is supported by the surface tension between a source rod and the crystalline material. In the process, the tip of the source rod is melted by the incidence of a high power CO_2 laser (10.6 μm), and a seed is put into contact with the melt. The seed and source rods are then raised to allow a new source into the focus of the laser, while single crystal material above the focus cools and solidifies. Such an experimental arrangement makes LHPG very advantageous when compared to other conventional growth methods such as Czochralski, because it eliminates the need for crucibles, which can be quite expensive for high melting point materials and also increases the chance of contamination. Another advantage is that single crystal fibres can be grown by LHPG in processes that are up to 60 times faster than large bulk crystals.

By employing LHPG, our group has succeeded in growing several single crystal fibre compositions, which are normally very difficult to obtain by other techniques [12, 15–17]. Most recently we have grown fibres of CaB_2O_6 oxide compounds where B = Nb or Ta [16, 17]. Despite the excellent optical quality with which such crystal fibres can be obtained, and the broad range of optical applications they could serve when doped with active ions such as neodymium, these oxides are traditionally studied as dielectric ceramics with applications in resonators at microwave frequencies (a few GHz), useful in mobile and satellite communications, in cellular phones and global positioning systems [18, 19]. Hence, there are very few reports on the growth and characterization of AB_2O_6 crystals [20, 21]. $CaTa_2O_6$ is a polymorphic oxide that exists in three different structural modifications depending on the temperature at which it is prepared. For high temperature synthesis, two structural modifications were identified: a tetragonal (α_1) phase stable from 1450 to 1650 °C, and a cubic (α_2) phase stable from 1650 °C to the melting point [22].

In this work we present the successful LHPG growth of undoped and neodymium (Nd^{3+}) doped $CaTa_2O_6$ single crystal fibres, along with a throughout spectroscopic characterization in the near infrared region, with the purpose of investigating their potential use in compact optical devices, such as near-infrared laser active media.

2. Experimental details

Undoped and Nd^{3+} doped (0.5–2.5 mol%) $CaTa_2O_6$ single crystal fibres were grown from pedestal rods (source and seed), using the LHPG equipment described elsewhere [14]. The pedestal rods were obtained by mixing stoichiometric amounts of the precursors $CaCO_3$ (Riedel

de Häen 99%), Nd_2O_3 (Merk 99.9%) and Ta_2O_5 (TEP 99.99%) with an organic ligand [14, 16]. The homogeneous mixtures were molded into cylindrical pedestal shapes with 1.0 mm diameter and 50 mm length, using a cold extrusion device. The green rods obtained were dried in air, and then used as seed and source in the growth process. Further details of fibres growth are given in [16].

X-ray diffraction patterns were measured in a Rigaku Rotaflex diffractometer model RU200B for the as-grown milled doped or undoped $CaTa_2O_6$ fibres using Cu Kα radiation. Raman scattering spectra were collected for undoped samples, using as an excitation source an Ar^+ laser (514.5 nm). The signal was filtered by a 0.85 m double monochromator and collected by a photomultiplier. Transmission spectra were measured longitudinally in a 0.27 cm length undoped fibre, in the spectral range of 4000–400 cm^{-1}, using a Nicolet Magna IR850 spectrophotometer equipped with a DTGS detector and a KBr beamsplitter.

The room temperature absorption spectra of doped samples were measured in the range 650–920 nm, using the same Nicolet spectrophotometer equipped with a Si detector and a quartz beamsplitter. The luminescence measurements were done at $T = 300$ K, in the range of 820 nm to 1.45 μm, using as an excitation source a diode laser at 808 nm. The signals were modulated by a chopper, filtered by a 0.3 m monochromator, collected by an InGaAs detector and amplified by a lock-in system. Excited state lifetime values were obtained from luminescence decay curves in time, which were measured with excitation at 800 nm by an optical parametric oscillator (OPO) system pumped by a YAG:Nd^{3+} laser.

Excited state absorption (ESA) measurements were done using a pump–probe experimental set up as described in [23]. The samples were pumped by a 14 Hz modulated Ti:sapphire laser at 808 nm and the probe radiation was provided by a broadband tungsten lamp modulated at 600 Hz. The signal was filtered by a 0.3 m monochromator and collected by a Ge detector. By taking the normalized difference in transmitted intensities I_p of the pumped crystal sample and I_u of the unpumped sample, one can relate to the ground state absorption (GSA), the stimulated emission (SE) and the excited state absorption cross sections (σ_{GSA}, σ_{SE} and σ_{ESA} respectively), the following way:

$$\frac{I_p(\lambda) - I_u(\lambda)}{I_p(\lambda)} = n_e \zeta L \left[\sigma_{GSA}(\lambda) + \sum_i \left(\frac{n_i}{n_e} \right) \left(\sigma_{SE,i} - \sigma_{ESA,i} \right) \right], \tag{1}$$

where n_e is the overall excited population, ζ is the amplification factor of the lock-in and L is the sample thickness, n_i/n_e is the ratio of populations in level i and the total density of excited ions. That way, the spectrum described by equation (1) is a combination of GSA, SE and ESA processes and its calibration in cross section units is done in regions where only ground state absorption or stimulated emission (and not ESA) are expected.

3. Results

The single crystal fibres of $CaTa_2O_6$ (doped or undoped) were successfully grown by LHPG with lengths up to 3 cm and typical diameters of 700 ± 11 μm. The fibres are all transparent and free of cracks and striations and their shape is cylindrical without any sign of faceting. The undoped samples are colourless but the doped ones present a slight blue colour. X-ray diffraction patterns and their refinements indicate that the fibres were grown with the cubic structure belonging to the $Pm3$ space group [24], and no secondary phases were detected. Figure 1 presents a photograph of a low doped (0.5 mol%) fibre.

The transmission spectrum of a 0.27 cm long undoped fibre is presented in figure 2(a). The weak absorption bands in this spectrum around 3.5 μm correspond to atmospheric CO_2

Figure 1. Photograph of a low doped (0.5 mol%) $CaTa_2O_6$:Nd^{3+} single crystal fibre grown by LHPG. The scale is in millimetres.

(This figure is in colour only in the electronic version)

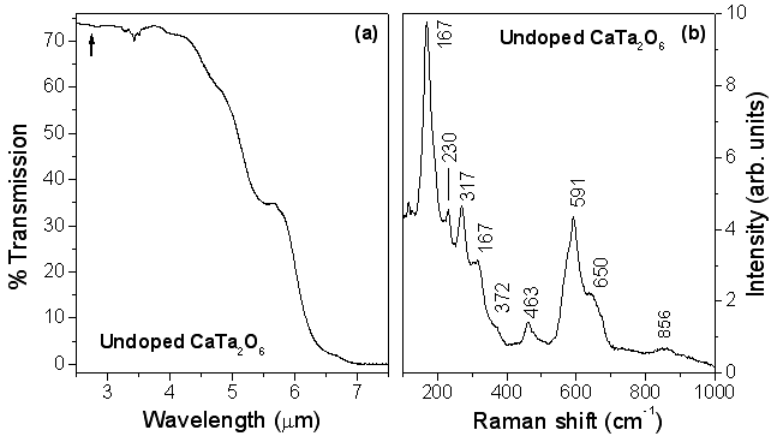

Figure 2. (a) Infrared transmission spectrum of an undoped 0.27 cm long $CaTa_2O_6$ single crystal fibre; (b) Raman scattering spectrum of the same undoped fibre obtained with excitation from an Ar^+ laser at 514.5 nm.

vibration modes. Figure 2(b) shows the Raman scattering spectrum of this same undoped fibre, and the peak values of the bands are indicated.

The room temperature ground state absorption spectrum of a 1.5 mol% Nd^{3+} doped fibre is presented in figure 3. The spectrum contains the typical bands of Nd^{3+} and the corresponding transitions are indicated. The inset shows the linear dependence of 808 nm band integrated intensities with Nd^{3+} concentration. Figure 4 displays the luminescence spectrum of the same 1.5 mol% doped fibre, which also contains the typical emission bands of Nd^{3+} at 890 nm, 1.06 and 1.34 μm. The corresponding transitions from level $^4F_{3/2}$ are indicated in the partial energy levels diagram, and the dependence of the integrated 1.06 μm emission band as a function of Nd^{3+} concentration is also shown in the inset. The average $^4F_{3/2}$ lifetime values were taken as those corresponding to a decrease of $1/e$ in luminescence intensity, and for the 0.5 mol% doped sample it is 200 μs.

Figure 5 brings the gain-ESA ($\sigma_{SE} - \sigma_{ESA}$) spectrum of a 0.5 mol% doped fibre and the transitions corresponding to the bands are indicated in the partial energy levels diagram. In

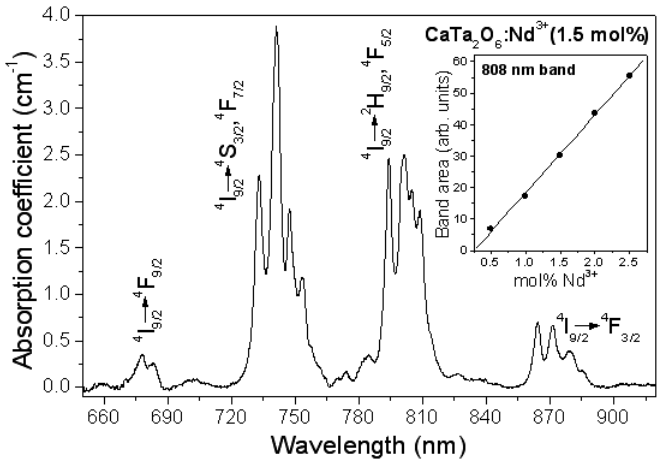

Figure 3. Room temperature ground state absorption spectrum of a 1.5 mol% Nd^{3+} doped $CaTa_2O_6$ single crystal fibre. The inset presents the curve of integrated intensity of the 808 nm absorption band as a function of increasing Nd^{3+} concentration and its linear fit.

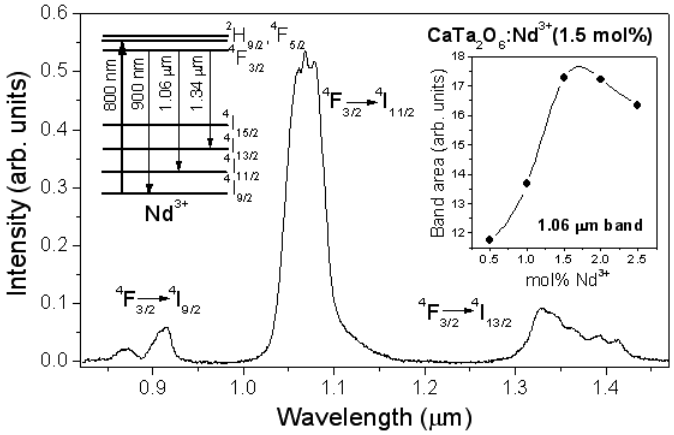

Figure 4. Room temperature luminescence spectrum of a 1.5 mol% Nd^{3+} doped $CaTa_2O_6$ single crystal fibre, obtained with excitation from a diode laser at 808 nm. The insets present the partial energy levels diagram indicating the corresponding transitions, and the 1.06 μm integrated emission band dependence on Nd^{3+} concentration.

the range of 950 nm to 1.45 μm no ground state absorption bands are observed, therefore only stimulated emissions and excited state absorptions from the $^4F_{3/2}$ state are observed.

4. Discussions

Once again the laser heated pedestal growth technique has proven to be an advantageous technique for the growth of high melting point crystals. The excellent optical quality of the $CaTa_2O_6$ crystal fibres, as shown in the photograph of figure 1, is confirmed by its transmission profile in figure 2(a). The transmission window extends up to 6.0 μm, and over 70% of the transmission is observed up to 4.5 μm. This is an important characteristic of the host crystal lattice, since it allows the study of the most important rare earth ions emissions in the near-infrared spectral region without interference of the host crystal. Also, the absence of

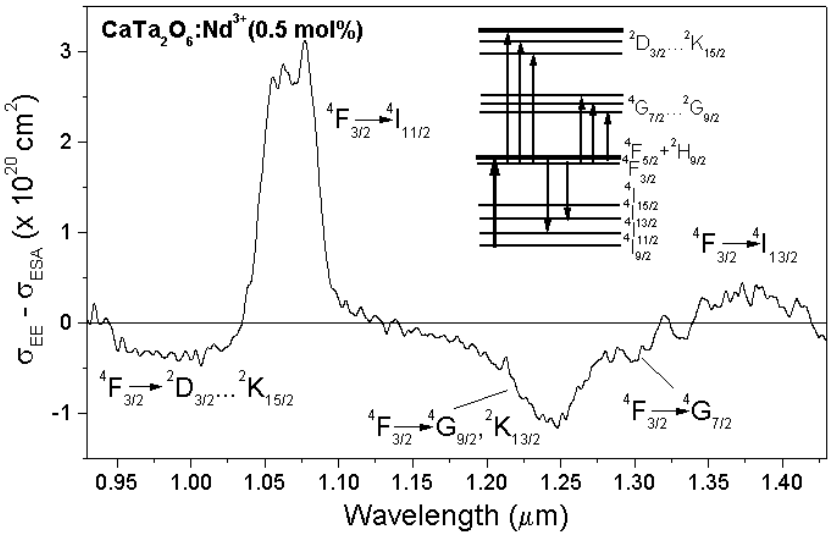

Figure 5. Gain-ESA spectrum of a 0.5 mol% Nd^{3+} doped $CaTa_2O_6$ single crystal fibre. The transitions from level $^4F_{3/2}$ are indicated in the partial energy levels diagram.

significant absorption around 3 μm due to OH^- vibrations, as indicated by the arrow, suggests that $CaTa_2O_6$ crystal fibres might also become an interesting host for Er^{3+} ions, with emission at 2.8 μm, of great interest for facial plastic surgery [25].

The formation of the stable cubic phase for all $CaTa_2O_6$ fibres, as confirmed by the x-ray diffraction patterns, is attributed to the high cooling rate ($\sim$1000 °C min^{-1}) associated with the experiments. The crystalline parameters obtained from Rietveld refinements of the patterns are $a = b = c = (7.757 \pm 0.002)$. This is also in accordance with the Raman spectrum presented in figure 2(b) that is considerably different from the one reported for the orthorhombic phase [26], when it comes to width and positions of bands. To the best of our knowledge, there are no reports of the Raman spectrum for the cubic phase, hence we have no means of attributing the bands to the vibration modes of the structure. However, we have found that from 100 to 450 cm^{-1}, some of the bands positions coincide with those of O–Ta–O bending vibrations of monoclinic Ta_2O_5 [27], and the bands at 167, 270, 243 and 650 cm^{-1} are also present in the spectrum of the orthorhombic phase, although with narrower linewidth. One reason for the apparent line broadening of Raman bands could be due to the fact that, since the fibres are rapidly cooled from the melt, there could be a significant amount of tensions in the metastable cubic structure, even though the fibres are not very fragile. As to the maximum phonon energy of $CaTa_2O_6$ fibres (856 cm^{-1}), it is comparable to those of well known laser crystals such as YAG:Nd^{3+} [28].

The inhomogeneous line broadening can also be verified in the absorption spectrum presented in figure 3. The full width at half maximum (FWHM) of the band at around 808 nm is 13 nm in contrast to 0.9 nm for the crystal of YAG:Nd^{3+}. Consequently, the apparent disadvantage of a smaller peak absorption cross section estimated for $CaTa_2O_6$:Nd^{3+} (1.5×10^{-20} cm^2) in comparison to YAG:Nd^{3+} (7.0×10^{-20} cm^2) [29] can be fully compensated for by the wider absorption of $CaTa_2O_6$:Nd^{3+}, depending on the desired application. When it comes to diode pumping at around 800 nm, for instance, the broadening is an advantageous characteristic, since it relaxes the need for temperature control of the diode laser to achieve best tuning conditions. Table 1 presents spectroscopic parameters of $CaTa_2O_6$:Nd^{3+} crystal

Table 1. Spectroscopic parameters of $CaTa_2O_6$:Nd^{3+} single crystal fibres in comparison to those of well known neodymium doped bulk laser crystals.

Nd^{3+} doped crystals	λ_{emis} (μm)	σ_{emis} (10^{-20} cm^2)	$FWHM_{emis}$ (nm)	σ_{abs} [a] (10^{-20} cm^2)	$FWHM_{abs}$ (nm)	τ_{rad} (μs)
$CaTa_2O_6$	1.068	3.0	45	1.5 (802 nm)	13	200
$Y_3Al_5O_{12}$ [29–31]	1.064	35	5.0	7.0 (808 nm)	0.9	230
$LiNbO_3$	1.085 (π)	27 (π)	2.6 (π)	8.7 (813 nm) (π)	4.0 (π)	108
[32, 33]	1.093 (σ)	7.5 (σ)	6.4 (σ)	6.7 (808 nm) (σ)	11 (σ)	

[a] Corresponds to maximum peak cross section of $^4I_{9/2} \rightarrow {}^2H_{9/2}, {}^4F_{5/2}$ transition band.

fibres in comparison to the well known Nd^{3+} doped YAG and $LiNbO_3$ crystals [29–33].

Still, another interesting aspect of the absorption spectra is that the intensities of the bands have a linear dependence with Nd^{3+} concentration, as can be seen in the inset of figure 3 for the band around 808 nm. This indicates that $CaTa_2O_6$ host fibres can efficiently incorporate up to 2.5 mol% Nd^{3+}, which is a fairly high doping concentration (2.0×10^{20} ions cm^{-3}), without compromising the optical quality of the fibres.

The luminescence spectrum in figure 4 shows the emission bands at around 900 nm ($^4F_{3/2} \rightarrow {}^4I_{9/2}$ transition), 1.06 μm ($^4F_{3/2} \rightarrow {}^4I_{11/2}$ transition), and 1.34 μm ($^4F_{3/2} \rightarrow {}^4I_{13/2}$). The $^4F_{3/2} \rightarrow {}^4I_{15/2}$ transition band is out of the measured spectral range. The bands at around 1.06 and 1.34 μm have FWHMs of 45 and 55 nm, respectively. These linewidths are also considerably larger than those of other bulk laser crystals as can be seen in table 1 for the band around 1.06 μm. The estimated peak emission cross section for this band is 3.0×10^{-20} cm^2, in contrast to 35×10^{-20} cm^2 for the YAG:Nd^{3+} crystal, however, similarly to the absorption spectrum, the low cross section of $CaTa_2O_6$:Nd^{3+} can be compensated for by its broader emission. In that sense, the fibres could find applications, for instance, as an active medium for compact pulsed or tunable lasers around 1.06 μm and other wavelengths.

The radiative lifetime value of 200 μs for excited state $^4F_{3/2}$ is assumed as that taken for the least doped fibre (0.5 mol%) in which ion–ion interactions are less probable. This value is of the same order of those for other laser crystals (see table 1). For a 2.5 mol% doped $CaTa_2O_6$:Nd^{3+} fibre, a decrease of 15% is observed in the lifetime value (170 μs). Although this decrease is not very critical to compromising the good energy storage capacity of level $^4F_{3/2}$, it can be attributed to the activation of energy transfer processes among ions, such as the cross relaxations $^4F_{3/2}, {}^4I_{9/2} \rightarrow {}^4I_{15/2}, {}^4I_{15/2}$ and $^4F_{3/2}, {}^4I_{9/2} \rightarrow {}^4I_{13/2}, {}^4I_{15/2}$ followed by non-radiative decay to the ground state $^4I_{9/2}$, and/or the energy migration $^4F_{3/2}, {}^4I_{9/2} \rightarrow {}^4I_{9/2}, {}^4F_{3/2}$ followed by non radiative losses in structural defects. Such energy transfer processes are also evidenced by a discrete quenching of luminescence intensity as the doping concentration is raised above ~1.5 mol%, as can be seen in the inset of figure 4 for the integrated intensity of the band around 1.06 μm.

The gain-ESA spectrum presented in figure 5 is a good indicator of the potentiality of $CaTa_2O_6$:Nd^{3+} single crystal fibres. Since no ESA is expected at around 1.06 μm, and the only metastable level is the $^4F_{3/2}$, the ratio n_i/n_e in equation (1) is 1 and therefore the calibration of the spectrum was done by imposing equality of the stimulated emission cross-sections of the $^4F_{3/2} \rightarrow {}^4I_{11/2}$ transition to the $(I_p - I_u)/I_p$ spectrum. The stimulated emission cross section was estimated by the Fuchtbauer–Lundenburg expression that relates the emission bandshapes and radiative lifetime to the emission cross sections [34].

From the spectrum it can be noted that the maximum ESA cross section at around 1.0 μm is 0.45×10^{-20} cm^2, and even if there is an overlap of this band (with smaller σ_{ESA}) with the

stimulated emission at 1.06 μm, it is evident that the ESA loss at this wavelength is negligible in comparison to the emission cross section of about 3.0×10^{-20} cm^2. Therefore the laser emission around 1.06 μm should not be compromised by ESA. However, at around 1.34 μm, the situation is just the opposite, the laser transition lies very close to a strong ESA band and taking bandwidths into consideration, the laser performance around this wavelength is strongly compromised by SE/ESA overlap.

5. Conclusions

High optical quality undoped and neodymium doped (0.5–2.5 mol%) $CaTa_2O_6$ single crystal fibres, with 700 μm diameter and up to 3 cm length, were grown for the first time by the laser heated pedestal growth technique. Analysis of x-ray diffraction and Raman scattering patterns indicate that all the fibres crystallized in the metastable cubic structure. The transmission window extends up to $\sim$6 μm and the maximum phonon energy of 856 cm^{-1} is comparable to those of well known bulk laser crystals. The absorption and emission peak cross sections are lower than those reported for YAG:Nd^{3+} and $LiNbO_3$:Nd^{3+} crystals but the spectral lines are much larger in $CaTa_2O_6$:Nd^{3+} and the radiative lifetime of level $^4F_{3/2}$ (200 μs) is comparable. The strongest evidence of the potentiality of the single crystal fibres as laser active media comes from the observation of stimulated emission around 1.06 μm ($\sigma_{SE} = 3.0 \times 10^{-20}$ cm^2), which is not compromised by ESA transitions. However, the stimulated emission at 1.34 μm is prevented by a strong overlap with an ESA band. To the best of our knowledge, this is the first report on the successful growth and spectroscopic characteristics of a $CaTa_2O_6$:Nd^{3+} single crystal fibre, which is a novel material that can become an interesting candidate for the construction of compact pulsed or tunable lasers.

Acknowledgments

Authors would like to thank the Brazilian agencies FAPESP and CNPq for financial support of this work.

References

[1] Zhang H, Chao M, Gao M, Zhang L and Yao J 2003 *Opt. Laser Technol.* **35** 445
[2] Moncorgé R, Chambon B, Rivoire J Y, Garnier N, Decroix E, Laporte P, Guillet H, Roy S, Mareschal J, Pelene D, Doury J and Farge P 1997 *Opt. Mater.* **8** 109
[3] Ermeneux F S, Goutadier C, Moncorgé R, Cohen-Adad M T, Betinelli M and Cavalli E 1997 *Opt. Mater.* **8** 83
[4] Mc Donald A V, Claffey N M, Pearson G J, Blau W and Setchell D J 2000 *Lasers Surg. Med.* **27** 213
[5] Tkachuk A M, Ivanova S E, Isaenko L I, Yelliseyev A P, Payne S, Solarz R, Page R and Nostrand M 2002 *Opt. Spectrosc.* **92** 83
[6] Zhang H J, Meng X, Zhu L, Wang C, Chow Y T and Lu M 2000 *Opt. Mater.* **14** 25
[7] Braunstein R 1955 *Phys. Rev.* **99** 1982
[8] Feigelson R S 1986 *J. Cryst. Growth* **79** 669
[9] Rudolph P and Fukuda T 1999 *Cryst. Res. Technol.* **34** 3
[10] Foulon G, Ferriol M, Brenier A, Cohen-Adad M-T, Boudeulle M and Boulon G 1997 *Opt. Mater.* **8** 65
[11] Ballman A A, Porto S P S and Yariv A 1963 *J. Appl. Phys.* **34** 3155
[12] de Camargo A S S, Nunes L A O, Ardila D R and Andreeta J P 2004 *Opt. Lett.* **29** 59
[13] Zayhowski J J 1999 *Opt. Mater.* **11** 255
[14] Hernandes A C 1999 *Recent. Res. Devel. Crystal Growth Res.* vol 1, ed Transworld Res. Network, Trivandrum, India p 123
[15] de Camargo A S S, Nunes L A O, Andreeta M R B and Hernandes A C 2002 *J. Phys.: Condens. Matter* **14** 13889
[16] Ferrari C R, de Camargo A S S, Nunes L A O and Hernandes A C 2004 *J. Cryst. Growth* **266** 475

[17] Silva R A A, de Camargo A S S, Cusatis C, Nunes L A O and Andreeta J P 2004 *J. Cryst. Growth* **262** 246
[18] Lee H-J, Kim I-T and Hong K S 1997 *Japan. J. Appl. Phys.* **36** L1318
[19] Kan A, Ogawa H and Ohsato H 2002 *J. Alloys Compounds* **337** 303
[20] Pólgar K, Péter A, Paitz J and Zaldo C 1995 *J. Cryst. Growth* **58** 365
[21] Ballman A A, Porto S P S and Yariv A 1963 *J. Appl. Phys.* **34** 3155
[22] Pivovarova A P, Strakhov V I and Smirnov Y N 1999 *Inorg. Mater.* **35** 1291
[23] Koetke J and Huber G 1995 *Appl. Phys.* B **61** 151
[24] Berndt M 1990–1995 *Inorg. Crystal Struct. Database. Retriev. 2.0*
[25] Kincade K 1999 *Laser Focus World* **35** 83
[26] Repelin Y, Husson E, Dao N Q and Brusset H 1979 *Spectrochim. Acta* A **35** 1165
[27] Dobal P S, Katiyar R S, Jiang Y, Guo R and Bhalla A S 2001 *Int. J. Inorg. Mater.* **3** 135
[28] Miller S E, Caspers H H and Rast H E 1968 *Phys. Rev.* **168** 964
[29] Jensen T, Ostroumov V G, Meyn J-P, Huber G, Zagumennyi A I and Shcherbakov I A 1994 *Appl. Phys.* B **58** 373
[30] Agnesi A, Pennacchio C, Reali G C and Kubecek V 1997 *Opt. Lett.* **22** 21
[31] Kück S, Fornasiero L, Mix E and Huber G 1998 *Appl. Phys.* B **67** 151
[32] Loro H, Voda M, Jaque F, García Sole J and Muñoz Santiuste J E 1995 *J. Appl. Phys.* **77** 5929
[33] Burlot R, Moncorgé R, Manaa H, Boulon G, Guyot Y, Garcia Solé J and Cochet-Muchy D 1996 *Opt. Mater.* **6** 313
[34] Miniscalco W J and Quimby R S 1991 *Opt. Lett.* **16** 258